

Regular article

Solvent effects on ^{17}O nuclear magnetic shielding: *N*-methylformamide in polar and apolar solutions

Maurizio Cossi, Orlando Crescenzi

Dipartimento di Chimica, Università Federico II, Complesso Monte S. Angelo, via Cintia, 80126 Naples, Italy

Received: 5 March 2003 / Accepted: 30 April 2003 / Published online: 24 February 2004
© Springer-Verlag 2004

Abstract. The solvent effect on ^{17}O isotropic shielding was computed by different methods: the polarizable continuum model and a mixed approach, including a few real solvent molecules treated as the solute. The experimental data show that the behavior of protic and aprotic solvents is markedly different: we found that the continuum approach describes well the observed shielding at various dielectric constants for aprotic solvents, while the mixed procedure is needed when hydrogen bonds to the magnetic centre are present.

Keywords: Polarizable continuum model – ^{17}O nuclear shielding – Discrete/continuum solvent models

1 Introduction

Electronic properties, as well as molecular energies and structures, are often deeply influenced by the environment [1, 2, 3, 4]. Since recent developments, especially in the field of density functional theory, greatly improved the theoretical calculation of NMR isotropic shieldings (and also coupling constants) [5, 6, 7], it has become important to account for solvent-induced shifts with the same accuracy. Several models have been proposed to include solute–solvent interactions in *ab initio* calculations [8, 9], one of the main contributions due to Jacopo Tomasi consisted in the development of the polarizable continuum model (PCM) [10], which is nowadays one of the most diffused and reliable approaches to compute solvent effects on energies, structures and properties.

Since 1981 the PCM has been continuously updated and extended [11, 12]: the most recent and complete formulation is presented in Ref. [13]; a further extension to second-order Møller–Plesset derivatives is presented

in another paper of the present volume [14]. While solvation free energies can be accurately computed by the PCM (provided the shape of the solute–solvent boundary is carefully defined) [15], it has been shown that some electronic properties are better described by a mixed approach, with a few solvent molecules explicitly treated at the same level as the solute, and the PCM used to add bulk solvent effects [16]. Some indications exist that also NMR shieldings should be treated by such a mixed approach, at least in solvents forming hydrogen bonds to the atoms whose nuclear shielding is computed (recent studies concentrated on ^{15}N and ^{17}O) [17, 18].

When a nucleus belonging to a molecular environment is placed in an external magnetic field, \vec{B}_{ext} , the surrounding electrons create an induced field, $\vec{B}_{\text{ind}} = -\sigma \cdot \vec{B}_{\text{ext}}$; the tensor σ reduces to a scalar ($\sigma = 1/3 \text{Tr}\sigma$, isotropic shielding constant) if the molecule is free to rotate, as in liquid solutions. The resulting local field acting on nuclei, $\vec{B}_{\text{local}} = (1 - \sigma)\vec{B}_{\text{ext}}$, can be weaker (shielding effect) or stronger (deshielding) than the external field, according to the sign of σ . In the quantum mechanical description, $\sigma - 1$ can be defined as the derivative of the molecular energy with respect to the external field and to the nuclear magnetic moment: effective procedures have been developed to compute this quantity at different levels of the theory [19]. Since this property is strongly dependent on the nuclear arrangement and on the electronic distribution, a strong effect from solute–solvent interactions is expected.

In the present work we computed the solvent shift of ^{17}O isotropic shielding in *N*-methylformamide (NMF), an important benchmark because it is the simplest peptide unit model. For this system, a number of experimental determinations exist [20, 21, 22, 23]: we refer to a series of NMR measurements in different solvents (spanning a wide range of polarity, with and without hydrogen bonds to the NMF oxygen) [22], in order to evaluate the reliability of the continuum and of the discrete/continuum approaches.

The NMR shielding solvent shifts are traditionally attributed to different effects at the molecular scale [24]; from our point of view, they can be divided into

Contribution to the Jacopo Tomasi Honorary Issue

Correspondence to: M. Cossi
e-mail: cossi@chemistry.unina.it

1. Solvent-induced deformation of the solute geometry, and possibly changes in vibrational motions involving the nucleus of interest ($\Delta\sigma_{\text{geom}}$).
2. Electrostatic polarization of the solute electronic distribution ($\Delta\sigma_{\text{polar}}$).
3. Nonelectrostatic short-range interactions involving molecules in the first solvation shells ($\Delta\sigma_{\text{vdw}}$).

We do not consider here the effect due to the solvent magnetic susceptibility, which can modify the local field experienced by the dissolved molecule: this is a “cooperative” effect which could hardly be modeled by *ab initio* calculations; anyway, experimental data are often corrected to take this effect into account by means of macroscopic models.

By definition, $\Delta\sigma_{\text{vdw}}$ can only be described by including explicit solvent molecules in the calculation (some attempts have been made to extend the continuum model by also incorporating a part of these effects [25], but such an approach is not implemented for NMR calculations). The other changes, $\Delta\sigma_{\text{geom}}$ and $\Delta\sigma_{\text{polar}}$, can be modeled both by the continuum and by the mixed procedure. However, the solute–solvent cluster geometry is usually optimized in some particular configurations (those expected to provide the greatest effect on the electronic property), and this will be unlikely to reproduce the global solvent effect on the solute geometry accurately: then we prefer to evaluate $\Delta\sigma_{\text{geom}}$ by the PCM. Another promising approach is to perform some kind of molecular dynamics simulation [17, 18, 26, 27], extracting a number of different solute–solvent clusters and averaging the results; a different route, based on the so-called averaged-solvent electrostatic potential, has also been proposed and applied to a number of chemical systems [28]. Of course, the reliability of this procedure depends on the quality of the potentials used in the simulation, anyway it has not been applied in this work.

We compared our calculations to a coherent series of experimental data, obtained in several solvents with different polarity [22]; since we are only interested in the solvent effect, all the data were referred to the least polar medium, i.e. carbon tetrachloride. Then we will not discuss the nuclear shielding absolute values, but rather the solvent shift in solvent S , that is the difference between the shielding measured or computed at the same level in solvent S and in CCl_4 :

$$\Delta\sigma(S) = \sigma(S) - \sigma(\text{CCl}_4) . \quad (1)$$

2 Methods

The calculations were performed at the density functional theory level, using a hybrid Kohn–Sham/Hartree–Fock approach derived from the Perdew, Burke and Ernzerhof functional (PBE), as reported in Ref. 29 (and known by the acronyms PBE0 or PBE1PBE): with this functional, nuclear shieldings in excellent agreement with experiment were obtained for a number of gaseous molecules [7]. The gauge-independent atomic orbitals (GIAO) [30] scheme was used to compute NMR constants; for both geometry optimizations and NMR constant calculations we adopted the 6-311+G(d,p) [31, 32] basis set, which was found to provide converged results in similar calculations [18].

For the continuum solvation model we used the last version of the PCM procedure [13]: following the original approach by Tomasi and coworkers, the solute is enclosed in a cavity modeled on its actual shape, and obtained by the envelope of spheres centered on solute atoms or atomic groups (hydrogens are included in the same sphere as the heavy atom they are bound to). In the present version, each heavy atom is assigned a radius which depends on the molecular topology (number of hydrogens attached, nature of first neighbors, molecular charge) [15]. Once the radii have been defined, they are multiplied by a “scaling factor” (f) which can be used to modify the total cavity volume keeping its shape. The radii and the scaling factor are optimized to provide hydration free energies in good agreement with experiment for a number of organic and inorganic molecules: in aqueous solution the usual scaling factor is $f = 1.2$; some authors found that in less polar solvents f has to be increased up to 1.4 to obtain good solvation energies [33].

The relative dielectric constant is 1 inside the cavity, and takes the bulk value immediately outside: as a consequence a solvation charge distribution appears on the cavity surface:

$$\Sigma(\mathbf{s}) = -\frac{\epsilon - 1}{4\pi\epsilon} E_n(\mathbf{s}) , \quad (2)$$

where \mathbf{s} is a point on the surface, Σ is the solvation charge density (in practice it is substituted by a pattern of point charges spread on the surface itself), ϵ is the solvent macroscopic dielectric constant, and $E_n(\mathbf{s})$ is the normal component of the electric field existing at point \mathbf{s} . The electric field comes from solute electrons and nuclei, from the surface solvation charge itself, and also from the volume solvation charge that should be added, owing to the fraction of solute electrons extending outside the cavity. This last contribution is the most difficult to calculate in practice. Recently it has been shown that the effect of the volume solvation charge can be very effectively reproduced by an additional surface charge, much easier to treat in actual implementations. Another useful feature of this approach, making the procedure computationally more convenient, is that the solvation charges depend on the solute electrostatic potential, rather than on the electric field.

On the basis of this model, a very efficient and robust procedure has been developed to include solvent effects on molecular energy and properties: the key steps are the definition of surface “tesserae”, i.e. finite elements where the charge density is discretized, the calculation of solvation charges

$$q(\mathbf{s}_i) = \sum_j Q_{ij} V(\mathbf{s}_j) \quad (3)$$

and of the PCM Fock-like operator

$$\begin{aligned} v^{\text{PCM}} &= \frac{1}{2} \frac{\partial}{\partial \rho} \sum_{i,j} V(\mathbf{s}_i) Q_{ij} V(\mathbf{s}_j) \\ &= \frac{1}{2} \sum_{i,j} \frac{\partial V(\mathbf{s}_i)}{\partial \rho} Q_{ij} V(\mathbf{s}_j) \\ &\quad + \frac{1}{2} \sum_{i,j} V(\mathbf{s}_i) Q_{ij} \frac{\partial V(\mathbf{s}_j)}{\partial \rho} \\ &= \sum_{i,j} V(\mathbf{s}_i) \left(\frac{Q_{ij} + Q_{ji}}{2} \right) \frac{\partial V(\mathbf{s}_j)}{\partial \rho} . \end{aligned} \quad (4)$$

Here \mathbf{s}_i and \mathbf{s}_j are points on the surface, ρ is the solute electronic density, V is the solute (electronic and nuclear) electrostatic potential, and Q_{ij} are elements of a geometric matrix connecting the different surface tesserae. Note that the definition of surface tesserae is analytic and differentiable, leading to the exact definition of energy gradients in solution. The PCM operator 4 can be used in the GIAO procedure for the calculation of NMR constants, including the electrostatic solute–solvent interactions in the result.

3 Results and discussion

The geometry of NMF (Fig. 1a) in vacuo and in nine solvents with different polarity was optimized at the

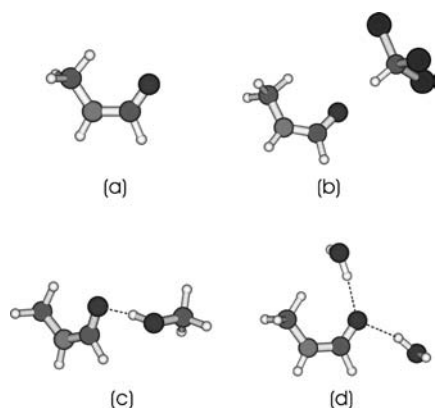


Fig. 1. Optimized structure of **a** *N*-methylformamide (NMF) in the gas phase, **b** NMF + CHCl₃ cluster in chloroform, **c** NMF + CH₃OH in methanol, **d** NMF + H₂O in water

PBE0/6-311+G(d,p) level using the PCM procedure. To investigate specific interactions with hydrogen-bonding solvents, we also optimized at the same level the structure of NMF · CHCl₃, NMF · CH₃OH, NMF · H₂O and NMF · (H₂O)₂ (Figs. 1b–d): in all the clusters the solvent acidic hydrogen points towards one of or both the lone pairs of the NMF oxygen; all the cluster optimizations were performed with the PCM (with the suitable dielectric constant) to add bulk effects too.

In all the optimized structures the OCNC moiety is planar, and the methyl group is arranged with one hydrogen almost eclipsed with respect to the carbonyl oxygen (the local NMF symmetry is nearly *C_s*). The main structural parameters in the various media, along with the computed ¹⁷O isotropic shielding, are reported in Table 1: here we did not include any solvent effect, apart from the geometry distortion. The main effect on the geometry, as expected, is the lengthening of the C=O bond and the corresponding shortening of the C–N bond; when explicit solvent molecules are included, these distortions are, in general, greater. From Table 1 it appears that the PCM $\Delta\sigma_{\text{geom}}$ is always negative and quite small for all the solvents (ranging from –0.6 to –3.2 ppm); at the cluster geometries, the $\Delta\sigma_{\text{geom}}$ values are still negative and greater in absolute value. Then the partial loss of the carbonyl oxygen *sp*² character, due to the solvent polarization, leads to a descreening effect, in contrast with the overall observed shift (see later).

Next, we evaluated the solvent shifts ($\Delta\sigma_{\text{geom}} + \Delta\sigma_{\text{polar}}$) with the PCM in the various solvents: as stated in the Introduction, the shifts are referred to CCl₄ (the least polar medium for which experimental data are available). The PCM calculations were repeated using different cavity scaling factors (see Methods). With a lower *f*, i.e. with a smaller cavity, the solvent effect is amplified; with the present choice of atomic radii, cavities with *f* < 1.0 are quite unphysical, because a significant fraction of solute electrons is found outside the cavity. The NMF ¹⁷O shieldings are reported, along with the corresponding solvent shifts in Table 2; the differences with respect to CCl₄ are also displayed in Fig. 2.

Two distinct experimental curves are clearly present, for protic and aprotic solvents, respectively: from Fig. 2 it is evident that the PCM reproduces well the behavior of aprotic solvents (using *f* = 1.4). On the other hand, with every scaling factor the PCM curves reach a plateau for $\epsilon \simeq 25$, while experimentally the solvent shift in water is markedly greater than that in methanol, for instance: this means that the correct trend cannot be reproduced for the protic solvents by the simple continuum model, with any cavity size. With the present atomic radii, the best solvation free energies in water are obtained with *f* = 1.2: some indications exist that in apolar solvents the scaling factor has to be increased to 1.4, though the PCM calculation of free energies in nonaqueous solvents is still not standardized. However, the data reported here show that in aprotic solvents the shifts are reproduced satisfactorily by the PCM with *f* = 1.4; using this scaling factor for aprotic, and *f* = 1.2 for protic solvents, one obtains the relative solvent shifts listed in Table 3.

Clearly, when a hydrogen bond can be formed to the NMF oxygen, the continuum approach is not sufficient to reproduce the whole effect: then we repeated the calculations on clusters containing one or two explicit solvent molecules. Such calculations were performed both on the isolated clusters (thus considering only the specific, short-range solute–solvent interactions) and embedding the clusters in the PCM (adding bulk effects too): the results are collected in Table 4, and displayed in Figs. 3, 4 and 5 for CHCl₃, methanol and water.

For the solvent chloroform, good agreement with the experimental relative shift is achieved using the PCM with *f* = 1.2 or a mixed approach, one explicit solvent molecule plus the PCM with *f* = 1.4. In this case, the solvating abilities of chloroform and carbon

Table 1. Main geometrical parameters (angstroms and degrees) in vacuo and in various solvents optimized with the polarizable continuum model (PCM), and NMR isotropic shielding (ppm) computed at the different geometries. No other solvent effects were included

Optimized in	<i>r</i> (C=O)	<i>r</i> (C–N)	∠(OCN)	σ
Gas phase	1.211	1.354	125.46	–65.1
CCl ₄	1.215	1.348	125.65	–65.7
Toluene	1.217	1.345	125.70	–65.8
CHCl ₃	1.222	1.343	125.78	–66.2
Acetone	1.226	1.339	125.85	–66.7
Ethanol	1.226	1.339	125.85	–66.8
Methanol	1.227	1.338	125.86	–66.8
CH ₃ CN	1.227	1.338	125.86	–68.1
Dimethyl sulfoxide	1.227	1.338	125.86	–68.2
Water	1.228	1.338	125.87	–68.4

Table 2. *N*-Methylformamide (NMF)¹⁷O isotropic shieldings (ppm) computed with PCM using different cavity scaling factors (*f*), and solvent shifts (ppm) with respect to carbon tetrachloride

Solvent	Dielectric constant	Isotropic shielding			Difference with respect to CCl ₄			Exp.
		<i>f</i> = 1.1	<i>f</i> = 1.2	<i>f</i> = 1.4	<i>f</i> = 1.1	<i>f</i> = 1.2	<i>f</i> = 1.4	
CCl ₄	2.23	-37.7	-43.1	-50.3				
Toluene	2.38	-35.8	-41.6	-49.2	1.9	1.5	1.1	3.7
CHCl ₃	4.90	-18.4	-27.8	-40.2	19.3	15.3	10.1	23.9
Acetone	20.70	-1.7	-14.7	-31.7	36.0	28.4	18.6	15.0
Ethanol	24.55	0.3	-13.4	-31.3	38.0	29.7	19.0	47.8
Methanol	32.63	1.7	-12.4	-30.7	39.4	30.7	19.6	53.1
CH ₃ CN	36.64	0.9	-12.7	-30.4	38.6	30.4	19.9	20.7
Dimethyl sulfoxide	46.70	1.6	-12.1	-30.0	39.3	31.0	20.3	22.8
Water	78.39	4.2	-10.4	-29.5	41.9	32.7	20.8	71.3

tetrachloride can be properly modulated by changing the cavity size, but this is no longer possible for more polar environments.

In methanol it is necessary to account both for specific and for long-range effects, to reproduce the observed shift. With two solvent molecules and the PCM (test not reported) the solvent effect was overestimated by about 5 ppm: the final conformation, however, was quite strained, owing to the steric hindrance of the two methanol molecules around the oxygen, and in actual solutions such a conformation is likely to occur rarely. On the other hand, in aqueous solution the best result is found with two water molecules bound to the oxygen, with additional bulk effects by the PCM. The final value is still slightly underestimated (by around 10 ppm); possibly, some other explicit molecules should be added to the cluster before embedding it in the PCM. An attractive approach to sample different solute-solvent conformations has recently been adopted for similar calculations [17, 18]: a molecular dynamics calculation is performed (either

with classical or ab initio intermolecular potentials) and a suitable number of frames are extracted, including more and more solvent molecules, until convergence is achieved. However, we note that for the present system remarkably good results are obtained with the simpler approach described earlier, using a single, optimized structure for the solute-solvent clusters.

It is also of interest to attribute the computed solvent shifts to electrostatic or nonelectrostatic (van der Waals) interactions: in the present version, the continuum model only accounts for electrostatics, whereas both interactions can be described by considering explicit solvent molecules. Since the two methods give results with the same sign and similar magnitude, one could argue that $\Delta\sigma_{\text{polar}}$ is dominating; however it remains to be determined if the differences between the continuum and the cluster plus-continuum approaches are due to a better description of electrostatics in the latter, or to a contribution from $\Delta\sigma_{\text{vdw}}$. To clarify this point, we repeated the calculation on the NMF · (H₂O)₂ cluster, substituting the solvent atoms with point charges, obtained by the Merz-Kollman procedure (i.e. fitting the electrostatic potential generated by the water molecules after removing the NMF). This procedure should provide a good estimate of the electrostatic interactions, excluding the van der Waals contribution. The ¹⁷O isotropic shielding was -20.8 ppm without the PCM, and +10.8 ppm when the “NMF plus point charges” system was embedded in the continuum: the values for the real cluster are -24.3 and +11.7 ppm, respectively. The corresponding solvent shifts with respect to CCl₄ are +29.5 ppm (without the PCM) and +61.1 ppm (with the PCM) for point charges, and +26.0 and +62.0 for real solvent molecules. The close similarity between the results obtained with point charges and with real molecules confirms that in this case the solvent shift is largely dominated by electrostatic interactions. One should remember, however, that here we are considering relative solvent shifts, referred to CCl₄: then a more correct conclusion is that the van der Waals contribution is quite similar in all the solvents that have been considered. The computed ¹⁷O shielding for isolated NMF is -65.1 ppm, while in CCl₄ with the PCM it is -50.3 ppm (Table 2), the electrostatic $\Delta\sigma_{\text{polar}}$ (CCl₄/gas phase) is then +14.8 ppm. If the experimental isotropic

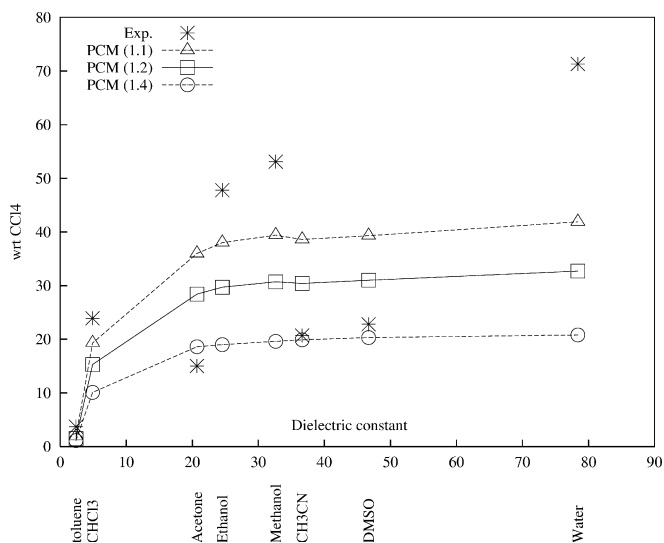
**Fig. 2.** Relative solvent shift (with respect to CCl₄, ppm) for NMF ¹⁷O nuclear shielding in different solvents: experimental data and polarizable continuum model calculations with various cavity scaling factors (Table 2)

Table 3. Relative solvent shifts on NMF ^{17}O isotropic shielding (ppm), computed with the PCM (cavity scaling factor 1.4 for aprotic and 1.2 for protic solvents). Reference value -50.3 ppm for CCl_4

Solvent	Dielectric constant	Solvent shift	Exp.
CCl_4	2.23		
Toluene	2.38	1.1	3.7
CHCl_3	4.90	22.5	23.9
Acetone	20.70	18.6	15.0
Ethanol	24.55	36.9	47.8
Methanol	32.63	37.9	53.1
CH_3CN	36.64	19.9	20.7
Dimethyl sulfoxide	46.70	20.3	22.8
Water	78.39	39.9	71.3

Table 4. Relative solvent shifts (ppm) for clusters with one or two solvent molecules, with and without bulk effects. Reference value -50.3 ppm for CCl_4

	CHCl_3	CH_3OH	H_2O
PCM only	22.5 ^a , 10.1 ^b	37.9	39.9
Cluster (one solvent molecule)	Isolated 6.5	7.8	7.3
	In the PCM 32.5 ^a , 24.2 ^b	52.4	53.6
Cluster (two solvent molecules)	Isolated		26.0
	In the PCM		62.0
Exp.	23.9	53.1	71.3

^a Cavity scaling factor 1.2

^b Cavity scaling factor 1.4

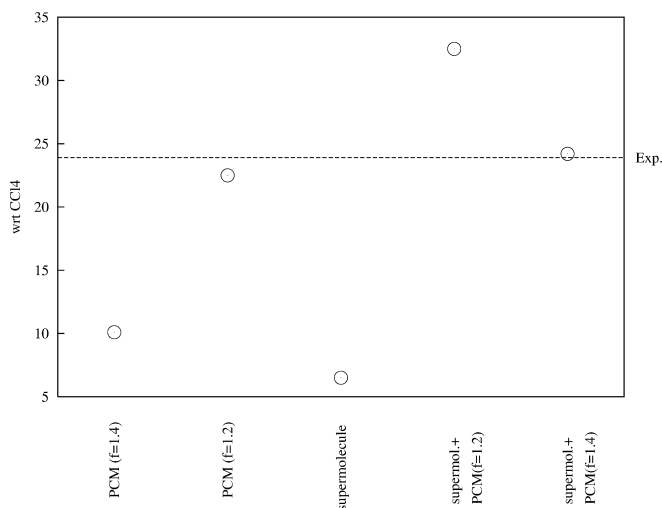


Fig. 3. NMF in chloroform: relative solvent shift (with respect to CCl_4 , ppm) computed with continuum, discrete and mixed solvent models (Table 4)

shielding in gas phase were available, one could estimate $\Delta\sigma_{\text{vdw}}$ by comparing this value to the total observed $\text{CCl}_4/\text{gas phase}$ shift.

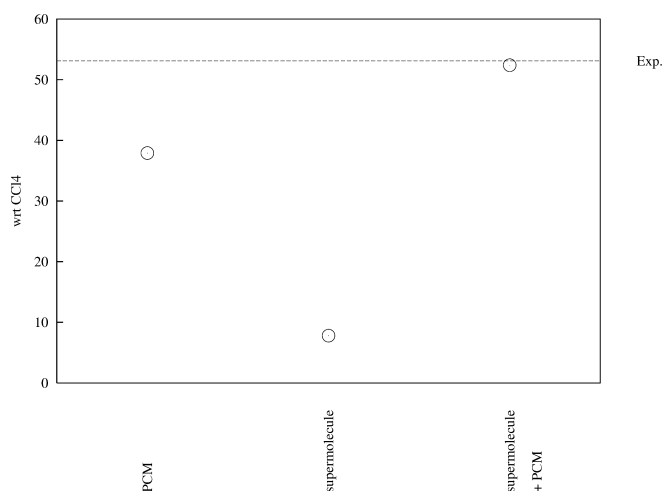


Fig. 4. NMF in methanol: relative solvent shift (with respect to CCl_4 , ppm) computed with continuum, discrete and mixed solvent models (Table 4)

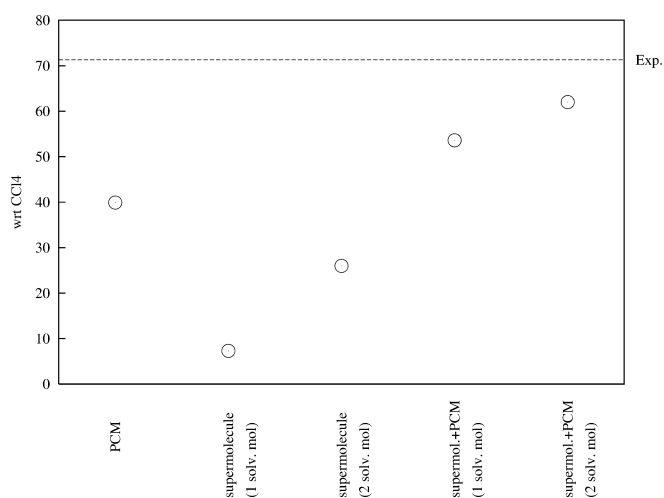


Fig. 5. NMF in water: relative solvent shift (with respect to CCl_4 , ppm) computed with continuum, discrete and mixed solvent models (Table 4)

4 Conclusions

The ^{17}O NMR nuclear shielding was calculated for NMF in a number of protic and aprotic solvents spanning a wide range of polarities. The solvent shifts (relative to the least polar medium, CCl_4) can be compared to a coherent series of experimental measures.

Two distinct experimental curves are present, referred to aprotic and protic solvents, respectively. We found that the solvent shifts in aprotic media are reproduced well by the PCM (using cavities scaled by a factor 1.4, to be compared to the factor 1.2 usually adopted for water). On the other hand, the PCM is not able to reproduce the experimental trend in protic solvents. Very satisfying results are obtained by a mixed approach, where one or two solvent molecules, hydrogen-bonded to the NMF oxygen, are treated explicitly and included in the “solute”. The explicit molecules account for

specific, short-range solute–solvent interactions, while bulk interactions are added by the PCM: both effects are necessary to obtain good agreement with experiment.

The relative solvent shifts seem to be essentially due to electrostatic interactions: the van der Waals contribution appears approximately constant for all the solvents we considered.

Acknowledgements. This work is dedicated to Jacopo Tomasi, to honor a career which has been fruitful in so many fields related to quantum chemistry. M.C. owes to Jacopo Tomasi his scientific education and his first steps in computational chemistry; we all are deeply indebted for Jacopo's human and scientific teaching.

References

1. Reichardt C (1990) Solvents and solvent effects in organic chemistry, 2nd edn. VCH, Weinheim
2. Rivail JL, Rinaldi D, Ruiz-Lopez MF (1995) In: Leszczynski J (ed) Computational chemistry: review of current trends. World Scientific, Singapore, pp
3. Cramer CJ, Truhlar DG (1996) In: Tapia O, Bertrán J (eds.) Solvent effects and chemical reactivity, Kluwer, Dordrecht, p 1
4. Adamo C, Cossi M, Rega N, Barone V (2001) In: Erikson LA (ed) Theoretical biochemistry: processes and properties of biological systems. Elsevier, Amsterdam, p 467
5. Malkin VG, Malkina OL, Salahub DR (1993) Chem Phys Lett 204: 87
6. Olsson L, Cremer D (1996) J Phys Chem 100: 16881
7. Adamo C, Cossi M, Barone V (1999) J Mol Struct (THEOCHEM) 493: 145
8. Tomasi J, Persico M (1994) Chem Rev 94: 2027
9. Cramer CJ, Truhlar DG (1999) Chem Rev 99: 2161
10. (a) Miertuš S, Scrocco E, Tomasi J (1981) Chem Phys 55: 117; (b) Cammi R, Tomasi J (1995) J Comput Chem 16: 1449; (c) Pascual-Ahuir JL, Silla E, Tomasi J, Bonaccorsi R (1987) J Comput Chem 8: 778
11. (a) Cossi M, Barone V, Cammi R, Tomasi J (1996) Chem Phys Lett 255: 327; (b) Amovilli C, Barone V, Cammi R, Cancès E, Cossi M, Mennucci B, Pomelli CS, Tomasi J (1998) Adv Quantum Chem 32: 227
12. (a) Cancès E, Mennucci B, Tomasi J (1997) J Chem Phys 107: 3032; (b) Mennucci B, Cancès E, Tomasi J (1997) J Phys Chem B 101: 10506; (c) Cossi M, Barone V (1998) J Chem Phys 109: 6246; (d) Mennucci B, Cammi R, Tomasi J (1999) J Chem Phys 110: 6858; (e) Cammi R, Mennucci B (1999) J Chem Phys 110: 9877; (f) Cossi M, Barone V (2001) J Chem Phys 115: 4708; (g) Cossi M, Rega N, Scalmani G, Barone V (2001) J Chem Phys 114: 5691
13. Cossi M, Scalmani G, Rega N, Barone V (2002) J Chem Phys 117: 43
14. Cammi R, Mennucci B, Pomelli C, Cappelli C, Corni S, Frediani L, Trucks GW, Frisch MJ (2004) Theor Chem Acc
15. Barone V, Cossi M, Tomasi J (1997) J Chem Phys 107: 3210
16. (a) Cossi M, Barone V (2000) J Chem Phys 112: 2427 (b) Improta R, Scalmani G, Barone V (2001) Chem Phys Lett 336: 349
17. Mennucci B, Martínez JM, Tomasi J (2001) J Phys Chem A 105: 7287
18. Cossi M, Crescenzi O (2003) J Chem Phys 118: 8863
19. Helgaker T, Jaszunski M, Ruud K (1999) Chem Rev 99: 293
20. Burgar MI, St Amour TE, Flat D (1981) J Phys Chem 85: 502
21. Gerothanassis IP, Vakka C (1994) J Org Chem 59: 2341
22. Diez E, San Fabian J, Gerothanassis IP, Esteban AL, Abboud J-LM, Contreras RH, de Kowalewski DG (1997) J Magn Reson 124: 8
23. de Kowalewski DG, Kowalewski VJ, Contreras RH, Diez E, Casanueva J, San Fabián J, Esteban AI, Galache ML (2001) J Magn Reson 148: 1
24. Buckingham AD, Schaefer T, Schneider WG (1960) J Chem Phys 32: 1227
25. Amovilli C, Mennucci B (1997) J Phys Chem B 101: 1051
26. Pfrommer BG, Mauri F, Louie SG (2000) J Am Chem Soc 122: 123
27. Cui Q, Karplus M (2000) J Phys Chem B 104: 3721
28. (a) Sanchez ML, Aguilar MA, Olivares del Valle FJ (1997) J Comput Chem 18: 313; (b) Sanchez ML, Aguilar MA, Martin ME, Olivares del Valle FJ (2000) J Comput Chem 21: 705; (c) Martin ME, Sanchez ML, Olivares del Valle FJ, Aguilar MA (2002) J Chem Phys 116: 1613
29. Adamo C, Barone V (1999) J Chem Phys 110: 6158
30. (a) Wolinski K, Hilton JF, Pulay P (1990) J Am Chem Soc 112: 8251; (b) Cheeseman JR, Trucks GW, Keith TA, Frisch MJ (1998) J Chem Phys 104: 5497
31. (a) McLean AD, Chandler GS (1980) J Chem Phys 72: 5639; (b) Krishnan R, Binkley JS, Seeger R, Pople JA (1980) J Chem Phys 72: 650
32. Frisch MJ, Pople JA, Binkley JS (1984) J Chem Phys 80: 3265
33. Luque FJ, Bachs M, Aleman C, Orozco M (1996) J Comput Chem 17: 806